Biosensors and Bioelectronics 28 (2011) 344–348

Contents lists available at ScienceDirect

Biosensors and Bioelectronics

journal homepage: www.elsevier.com/locate/bios

A new preparation of Au nanoplates and their application for glucose sensing

Yingwei Zhang[a], Guohui Chang[a], Sen Liu[a], Wenbo Lu[a], Jingqi Tian[a,b], Xuping Sun[a,*]

[a] State Key Lab of Electroanalytical Chemistry, Changchun Institute of Applied Chemistry, Changchun 130022, Jilin, PR China
[b] Chinese Academy of Sciences, Graduate School of the Chinese Academy of Sciences, Beijing 100039, PR China

ARTICLE INFO

Article history:
Received 27 May 2011
Received in revised form 17 July 2011
Accepted 18 July 2011
Available online 22 July 2011

Keywords:
Au nanoplate
Tannic acid
Glucose biosensor
Human blood serum

ABSTRACT

The present communication demonstrates a relatively green preparative route toward Au nanoplates in aqueous solution at room temperature with the use of tannic acid (TA), which is an environmentally friendly, soluble polyphenol, as a reducing agent. Such Au nanoplates exhibit notable catalytic performance toward the oxidation and reduction of H_2O_2. A glucose biosensor was further fabricated by immobilizing glucose oxidase (GOD) into chitosan–Au nanoplate composites film on the surface of glassy carbon electrode (GCE). This sensor exhibits good response to glucose, and the linear response range is estimated to be from 2 to 20 mM (R = 0.999) at 0.65 V and from 2 to 10 mM (R = 0.993) at −0.2 V, respectively. The sensitivity of the sensor determined from the slopes is 49.5 μA mM^{-1} cm^{-2} at 0.65 V.

1. Introduction

Metal nanostructures have attracted considerable attention in recent years due to their unique chemical and physical properties that are distinctly different from their bulk counterparts, and have been broadly used in catalysis (Yin et al., 2011; Somorjai, 1996), photonics (Sardar et al., 2009; Yavuz et al., 2009), electronics (Jeong et al., 2008), biosensing (Liu and Lu, 2003; Pingarron et al., 2008) and nanomedicines (Chen et al., 2007; Jain et al., 2007). Currently, many efforts have been made to develop various synthesis methods of metal nanoparticles with control morphologies (Capek, 2004; Chen and Holt-Hindle, 2010; Lee et al., 2001; Li et al., 2011; Yin et al., 2003). However, most of the methods reported relied heavily on organic solvents and environmentally and biologically hazardous reducing agents (Chou and Ren, 2000; Leopold and Lendl, 2003; Lee et al., 2008; Murphy et al., 2005; Tan et al., 2003). Hence, there is an increased interest on the development of a green synthetic strategy, which is designed to reduce or eliminate the use and generation of hazardous substances in synthetic processes (Anastas and Williamson, 1996; Desimone, 2002; Poliakoff and Anastas, 2001; Poliakoff et al., 2002).

Au nanomaterials have been widely used in biomedical fields due to their excellent biocompatibility, nontoxicity, catalytic activity and offer a hospitable environment for biomolecules (Jain et al., 2008; Rosi and Mirkin, 2005; Schmid, 1992). Hence, there is increasing research attention to biosensors based on Au nanomaterials (Daniel and Astruc, 2004; Melancon et al., 2008). Compared with other sensors, electrochemical biosensors have attracted tremendous attention because of their fast detection, low cost, high sensitivity, and good selectivity toward many analytes (Ahmed et al., 2008; Drummond et al., 2003). Au nanoparticles have advantages for the preparation of electrochemical biosensors with enhanced analytical performance, due to providing a stable immobilization of biomolecules retaining their bioactivity and facilitating electron transfer between the immobilized proteins and electrode substrates (Pingarron et al., 2008; Shan et al., 2010). Although Au nanoparticle based electrochemical biosensing has been largely studied (Claussen et al., 2009; Jia et al., 2008; Li et al., 2007), little attention has been paid to electrochemical sensing application of two-dimensional Au nanoplates (Seo et al., 2011).

Tannic acid (TA, Fig. S1) as a water-soluble, phenolic hydroxyl-rich compound is widely present in woods such as oak, walnut and mahogany and has been used as common mordant in industry. To the best of our knowledge, however, the use of TA as a reducing agent for the preparation of Au nanomaterials has not been explored so far. In this communication, we report on our recent finding that Au nanoplates can be successfully prepared on a large scale through a green, cost-effective and environmentally friendly strategy with the use of TA as a reducing agent. We further construct a glucose biosensor with the use of such Au nanoplates as building blocks and demonstrate successfully its application for glucose detection in both buffer and human blood serum.

2. Experimental

2.1. Materials

H_2O_2 (30 wt%), glucose, TA, Na_2HPO_4, and NaH_2PO_4 were purchased from Aladin Ltd. (Shanghai, China). Glucose oxidase (GOD)

* Corresponding author. Tel.: +86 431 85262065; fax: +86 431 85262065.
E-mail address: sunxp@ciac.jl.cn (X. Sun).

0956-5663/$ – see front matter © 2011 Elsevier B.V. All rights reserved.
doi:10.1016/j.bios.2011.07.041

(molecular weight: 160 kDa) and $HAuCl_4$ were purchased from Aldrich Chemical Comp. All chemicals were used as received without further purification. The water used throughout all experiments was purified through a Millipore system. Phosphate buffer saline (PBS) was prepared by mixing stock solutions of NaH_2PO_4 and Na_2HPO_4 and a fresh solution of H_2O_2 was prepared daily. Human blood serum was obtained form Institute of Virology and AIDS Research, First Affiliated Hospital, Jilin University, Changchun, Jilin, People's Republic of China.

2.2. Preparation of Au nanoplates using TA as a reducing agent

In a typical experiment, 40 μL of 5 mg/mL TA aqueous solution was diluted by 500 μL of water, and then 100 μL of 24.3 mM $HAuCl_4$ aqueous solution was added into the above diluted TA solution at room temperature. After a few minutes, an obvious color change from light yellow to golden brown occurred, leading to a large amount of sand-like precipitates. The resultant precipitates were centrifuged and washed with distilled water twice and redispersed in water for characterization and further use. Furthermore, the control experiments of changing the concentration and proportion of TA and $HAuCl_4$, respectively, reaction temperature, and pH value were also performed.

2.3. Fabrication of Au nanoplate-modified glassy carbon electrode (GCE)

The modified electrodes were prepared by a simple casting method. Prior to the surface coating, the GCE was polished with 1.0 and 0.3 μm alumina powder, respectively, and rinsed with doubly distilled water, followed by sonication in ethanol solution and doubly distilled water successively. Then, the electrode was allowed to dry in a stream of nitrogen. To obtain the Au nanoplate-modified GCE, 3 μL of the TA-reduced Au nanoplates dispersion (the Au concentration of the sample is 4 mM) was dropped on the clean surface of GCE, and then 2 μL chitosan (0.5%) solution was also dropped for stabilizing it. Finally, the electrode was allowed to dry in ambient air to obtain chitosan/Au nanoplate/GCE. The chitosan/TA/GCE was also prepared by the same method for the control experiments. Next, for the experiments of glucose detection, the chitosan/GOD/Au nanoplate/GCE was also prepared by the same method except for an extra dropping of 3 μL GOD (40 mg/mL), and then the electrode was dried at 4 °C for 2 h.

2.4. Characterization

Transmission electron microscopy (TEM) measurement was made on a HITACHI H-8100 EM (Hitachi, Tokyo, Japan) with an accelerating voltage of 200 kV. Scanning electron microscopy (SEM) measurements were made on a XL30 ESEM FEG scanning electron microscope at an accelerating voltage of 20 kV. Powder X-ray diffraction (XRD) data were recorded on a Rigaku D/MAX 2550 diffractometer with Cu Kα radiation (λ = 1.5418 Å). Electrochemical measurements are performed with a CHI 660D electrochemical analyzer (CH Instruments, Inc., Shanghai). A conventional three-electrode cell was used, including a GCE (geometric area = 0.07 cm^2) as the working electrode, a Ag/AgCl (saturated KCl) electrode as the reference electrode, and platinum foil as the counter electrode. The potentials are measured with a Ag/AgCl electrode as the reference electrode. All the experiments were carried out at ambient temperature.

3. Results and discussion

Fig. 1a and b shows the TEM images of the precipitates thus formed. It is seen that well-defined nanoplates with triangular and hexagonal morphologies are obtained, with the edge lengths mainly ranging from 400 to 700 nm. Fig. 1c shows typical SEM images, further indicating the formation of nanoplates about 18 nm in thickness (inset). Some nanoparticles are also noticed as by-products in the same sample. The crystalline nature of these nanoplates was further confirmed by the corresponding X-ray diffraction pattern (Fig. 1d). The five sharp peaks can be assigned to the (1 1 1), (2 0 0), (2 2 0), (3 1 1), and (2 2 2) diffraction peaks of metal Au, respectively, indicating that the precipitate is composed of crystalline Au. Note that the intensity ratio between (2 0 0) and (1 1 1) diffraction peaks is lower than the standard file (JCPDS) (0.18 versus 0.33). These observations confirm that our nanoplates are primarily dominated by (1 1 1) facets, and thus, their (1 1 1) planes tend to be preferentially oriented parallel to the surface of the supporting substrate (Sun et al., 2004, 2005). However, owing to the coexistence of Au nanoparticles on the supporting substrate, the intensity ratio of (2 0 0) versus (1 1 1) is not very small (Umar and Oyama, 2006). The spontaneous formation of Au nanoplates in our present study can be attributed to the direct redox between TA and Au^{3+}, where Au^{3+} is reduced to metallic Au by the phenolic hydroxyls of TA. Indeed, bayberry tannin as a phenolic hydroxyl-rich compound has recently been successfully used as a reducing agent and stabilizing agent for the synthesis of Au nanoparticles and Pd nanoparticles (Huang et al., 2009, 2010). Furthermore, the control experiments of changing the concentration and proportion of TA and $HAuCl_4$ respectively, reaction temperature, and pH value were also performed, and the morphologies of corresponding Au nanostructured products have been shown in Fig. S2. It is seen that the products are almost nanoparticles when increasing the proportion of TA and $HAuCl_4$ to two times of initial value (Fig. S2a), and relatively thinner nanoplates with small nanoparticles are obtained when decreasing the proportion of TA and $HAuCl_4$ to 1/2 of initial value (Fig. S2b). When increasing the concentration of TA and $HAuCl_4$ to two times of initial concentration, relatively thicker Au nanoplates as main product are observed (Fig. S2c). When decreasing the concentration of TA and $HAuCl_4$ to 1/2 of initial concentration, only small nanoparticles are observed (Fig. S2d). Besides, when increasing the reaction temperature to 70 °C or increasing the pH value of reaction system by adding 3 μL of 1 M NaOH, only nanoparticles can be obtained (Fig. S2e and f). Hence, Au nanoplates as main products can be obtained by controlling the proportion and concentration of TA and $HAuCl_4$. The products were then subjected to centrifugation at 3000 rpm for 2 min to collect Au nanoplates. The percentage of Au nanoplates in products was estimated to be 70 wt% from further drying-weighing procedure.

To demonstrate the sensing application of such Au nanoplates, we first constructed an enzymeless H_2O_2 sensor by immobilizing Au nanoplate with chitosan on a GCE surface. Fig. 2 shows the electrocatalytic responses of bare GCE, chitosan/TA/GCE, and chitosan/Au nanoplate/GCE in 0.2 M PBS at pH 7.4 in the presence of 2 mM H_2O_2. It is seen that the responses of both the bare GCE and chitosan/TA/GCE toward H_2O_2 are quite weak. In contrast, the chitosan/Au nanoplate/GCE exhibits notable catalytic current in the process of both oxidation and reduction of H_2O_2. It is also important to note that the chitosan/Au nanoplate/GCE exhibits no electrochemical response in the absence of H_2O_2. All these observations indicate that such Au nanoplates exhibit notable electrocatalytic activity toward the oxidation and reduction of H_2O_2. The relative standard deviation (RSD) of the amperometric response to 2 mM H_2O_2 is 4.1% for 5 successive measurements, indicating the good reproducibility of the chitosan/Au nanoplate/GCE.

It is well known that diabetes mellitus is a worldwide public health problem and thus the detection of glucose in blood serum is particularly important (Toghill and Compton, 2010). Based on the high electrocatalytical activity of chitosan/Au nanoplate/GCE

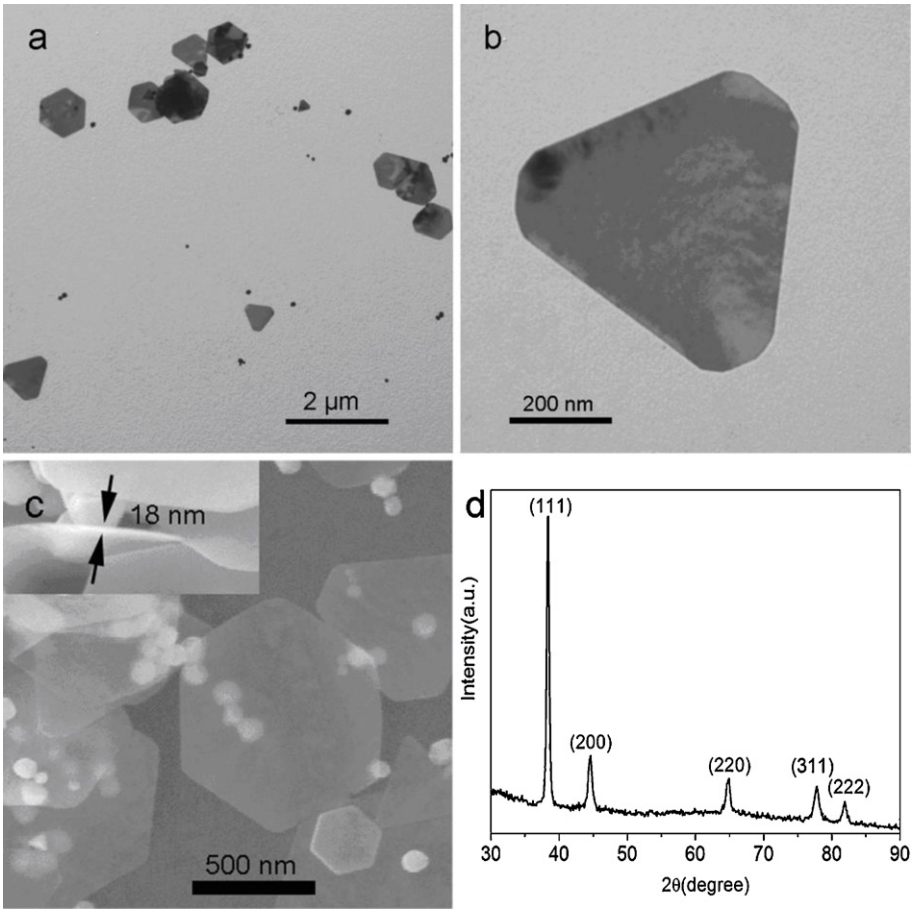

Fig. 1. (a and b) TEM images, (c) SEM image, and (d) XRD pattern of the precipitates. The inset in (c) shows that the thickness of a single nanoplate is about 18 nm.

toward H_2O_2, a glucose sensor was further developed by immobilizing GOD into chitosan–Au nanoplate composites film on a GCE surface. The sensing mechanism is that GOD can selectively catalyze the oxidation of glucose in the presence of oxygen to form H_2O_2, which can be electrochemically detected (Jia et al., 2010; Tsai and Tsai, 2009). Fig. 3a shows the cyclic voltammograms of the chitosan/GOD/Au nanoplate/GCE in 0.2 M PBS solution at pH 7.4 with various concentrations of glucose in saturated O_2. It is seen that a strong reduction current peak at −0.2 V is observed,

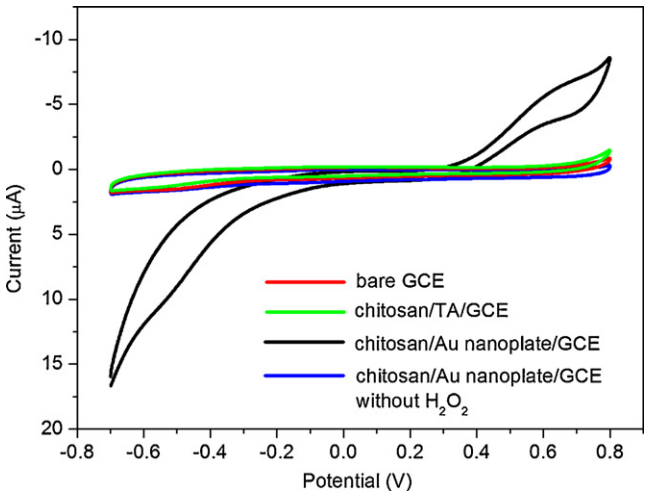

Fig. 2. Cyclic voltammograms of different electrodes in N_2-saturated 0.2 M PBS at pH 7.4 in the presence of 2 mM H_2O_2 (scan rate: 50 mV/s).

which is attributed to the electrochemical reduction of O_2 and H_2O_2, and a strong oxidation current peak at 0.65 V is also observed, which is attributed to the electrochemical oxidation of H_2O_2. It is also found that both the oxidation current at positive potential and the reduction current at negative potential increase with the increased amount of glucose in saturated O_2. Fig. 3a inset shows the calibration curves to corresponding amperometric responses at 0.65 V and −0.2 V, respectively. Good linear relationships are observed between the catalytic current and glucose concentration at ranges from 2 to 20 mM (R = 0.999) at 0.65 V and from 2 to 10 mM (R = 0.993) at −0.2 V. The sensitivity of the sensor determined from the slopes is 49.5 μA mM^{-1} cm^{-2} at 0.65 V, and the detection limit at 0.65 V is estimated to be 200 μM at a signal-to-noise ratio of 3. Compared to the sensitivity (15.17 μA mM^{-1} cm^{-2}) of one-dimensional Au nanorods (Li et al., 2010), this Au nanoplate-based sensor exhibits higher sensitivity. The RSD of the current response to 6 mM glucose at 0.65 V and −0.2 V are 4.5% and 4.0% for 5 successive measurements, respectively. Compared to the RSD (5.2%) of the Pt nanoparticle-based glucose biosensor (Kang et al., 2008) and the RSD (5.1%) of the Au nanorod-based glucose sensor, our Au nanoplate-based sensor has better reproducibility. Many reports (Chen et al., 1996; Katz et al., 2004; Shi and Ma, 2010) have given some evidence that the surface of nanomaterials would facilitate the immobilization of enzyme, and improve the activity and stability of the enzyme. In our system, the excellent performance of the biosensor may be attributed to that Au nanoplates adsorb GOD molecules effectively due to their large specific surface area promoting electron transfer between GOD and the surface of electrodes. All the above results indicate that our Au nanoplates-based glucose sensor has higher sensitivity and wider linear range,

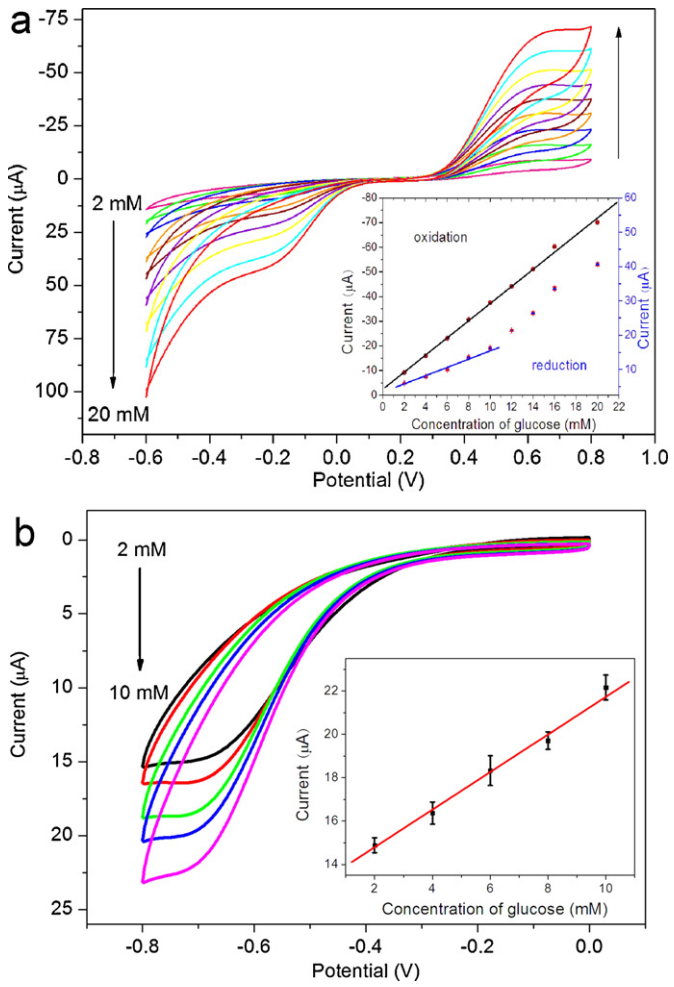

Fig. 3. (a) Cyclic voltammograms of chitosan/GOD/Au nanoplate/GCE in O_2 saturated 0.2 M PBS at pH 7.4 in various concentrations of glucose. Inset is the calibration curves corresponding to amperometric responses at 0.65 V and −0.2 V, respectively. (b) Cyclic voltammograms of chitosan/GOD/Au nanoplate/GCE in O_2 saturated 1.5 mL real blood serum sample and 3.5 mL PBS solution (0.2 M, pH 7.4) in the presence of various concentrations of glucose: 2, 4, 6, 8, and 10 mM. Inset is the calibration curve (R = 0.995) corresponding to amperometric responses at the reduction peak (scan rate: 50 mV/s).

and the detailed comparison of our present work with others regarding the performance of the glucose assays is summarized in Table S1.

The interference from common interference species such as dopamine (DA), ascorbic acid (AA), and uric acid (UA) was also investigated by using their relevant physiological levels (0.1 mM) (Guo et al., 2010). Fig. S3 shows the amperometric responses of chitosan/GOD/Au nanoplate/GCE toward 2 mM glucose in the absence and presence of the interference species at −0.2 V. It is seen that the injections of these interferences into 2 mM glucose show negligible responses.

Since the blood glucose levels of normal persons are in the range of 4 to 6 mM (Shan et al., 2010), our glucose biosensor may be used for glucose determination of real samples due to its wide linear response ranges. The original glucose concentration of the human blood serum sample is 6.10 mM (the detection result is provided by Institute of Virology and AIDS Research). The electrolyte solution containing 1.5 mL of serum sample and 3.5 mL phosphate buffer solution (0.2 M, pH 7.4) is used for cyclic voltammetric experiment. The reduction peak current increases with successive addition of 2 mM glucose into the blood serum saturated with O_2, as shown in Fig. 3b. Fig. 3b inset shows that the peak currents increase linearly with increased glucose concentrations saturated with O_2 (R = 0.995). The RSD of the current response to 6 mM glucose is 4.6% for 5 successive measurements.

The long-term stability of the prepared glucose biosensor is a critical factor in practical detection application. To evaluate the stability of this glucose biosensor, the chitosan/GOD/Au nanoplate/GCE was stored at 4 °C. The stability was examined by periodical measurements of the biosensor responses to 2 mM glucose in PBS solution (pH 7.4) at a scan rate of 50 mV/s. The variation of the response current at the chitosan/GOD/Au nanoplate/GCE decreases to about 91% of its initial response current on the 2nd day and about 79% on the 5th day, as shown in Fig. S4a. The loss of the response current could be ascribed to the decrease of the enzyme activity during these days. We also performed a control experiment using a dissolved GOD solution without its immobilization on the electrode, as shown in Fig. S4b. It is seen that the immobilized GOD exhibits relatively higher stability compared to GOD in solution, and this can be attributed to a favourable enzyme–substrate affinity in which more immobilized enzyme remains in an active conformation (He et al., 2010).

4. Conclusions

Mixing aqueous TA and $HAuCl_4$ solutions at room temperature has been proven to be an effective route toward green preparation of Au nanoplates. It suggests such Au nanoplates show notable catalytic performance toward the oxidation and reduction of H_2O_2. The use of such Au nanoplates as building blocks for the construction of biosensor for glucose detection in both buffer and human blood serum has also been demonstrated successfully. This sensor is promising for glucose determination of real samples.

Appendix A. Supplementary data

Supplementary data associated with this article can be found, in the online version, at doi:10.1016/j.bios.2011.07.041.

References

Ahmed, M.U., Hossain, M.M., Tamiya, E., 2008. Electroanalysis 20, 616–626.
Anastas, P.T., Williamson, T.C., 1996. Green Chemistry: Designing Chemistry for the Environment, first ed. American Chemical Society.
Capek, I., 2004. Adv. Colloid Interface Sci. 110, 49–74.
Chen, A.C., Holt-Hindle, P., 2010. Chem. Rev. 110, 3767–3804.
Chen, J.Y., Wang, D.L., Xi, J.F., Au, L., Siekkinen, A., Warsen, A., Li, Z.Y., Zhang, H., Xia, Y.N., Li, X.D., 2007. Nano Lett. 7, 1318–1322.
Chen, Z.J., Ou, X.M., Tang, F.Q., Jiang, L., 1996. Colloids Surf. B 7, 173–179.
Chou, K.S., Ren, C.Y., 2000. Mater. Chem. Phys. 64, 241–246.
Claussen, J.C., Franklin, A.D., Haque, A., Porterfield, D.M., Fisher, T.S., 2009. ACS Nano 3, 37–44.
Daniel, M.C., Astruc, D., 2004. Chem. Rev. 104, 293–346.
Desimone, J.M., 2002. Science 297, 799–803.
Drummond, T.G., Hill, M.G., Barton, J.K., 2003. Nat. Biotechnol. 21, 1192–1199.
Guo, C.X., Sheng, Z.M., Shen, Y.Q., Dong, Z.L., Li, C.M., 2010. ACS Appl. Mater. Interfaces 2, 2481–2484.
He, P., Greenway, G., Haswell, S., 2010. Microfluid Nanofluid 8, 565–573.
Huang, X., Wang, Y.P., Liao, X.P., Shi, B., 2009. Chem. Commun., 4687–4689.
Huang, X., Wu, H., Liao, X.P., Shi, B., 2010. Green Chem. 12, 395–399.
Jain, P.K., El-Sayed, I.H., El-Sayed, M.A., 2007. Nano Today 2, 18–29.
Jain, P.K., Huang, X., El-Sayed, I.H., El-Sayed, M.A., 2008. Acc. Chem. Res. 41, 1578–1586.
Jeong, S., Woo, K., Kim, D., Lim, S., Kim, J.S., Shin, H., Xia, Y., Moon, J., 2008. Adv. Funct. Mater. 18, 679–686.
Jia, F., Shan, C.S., Li, F.H., Niu, L., 2008. Biosens. Bioelectron. 24, 945–950.
Jia, W., Wang, K., Xia, X., 2010. Trends Anal. Chem. 29, 306–318.
Kang, X., Mai, Z., Zou, X., Cai, P., Mo, J., 2008. Talanta 74, 879–886.
Katz, E., Willner, I., Wang, J., 2004. Electroanalysis 16, 19–44.
Lee, C.L., Wan, C.C., Wang, Y.Y., 2001. Adv. Funct. Mater. 11, 344–347.
Lee, Y., Choi, J.R., Lee, K.J., Stott, N.E., Kim, D., 2008. Nanotechnology 19, 415604.
Leopold, N., Lendl, B., 2003. J. Phys. Chem. B 107, 5723–5727.
Li, J.W., Yu, J.J., Zhao, F.Q., Zeng, B.Z., 2007. Anal. Chim. Acta 587, 33–40.
Li, Y., Wang, X.X., Dong, X., He, Z.P., Zhang, H.Q., 2010. Rare Metals 29, 238–242.
Li, Y., Zaluzhna, O., Xu, B.L., Gao, Y., Modest, J.M., Tong, Y.J., 2011. J. Am. Chem. Soc. 133, 2092–2095.

Liu, J.W., Lu, Y., 2003. J. Am. Chem. Soc 125, 6642–6643.
Melancon, M.P., Lu, W., Yang, Z., Zhang, R., Cheng, Z., Elliot, A.M., Stafford, J., Olson, T., Zhang, J.Z., 2008. Mol. Cancer Ther. 7, 1730–1739.
Murphy, C.J., San, T.K., Gole, A.M., Orendorff, C.J., Gao, J.X., Gou, L., Hunyadi, S.E., Li, T., 2005. J. Phys. Chem. B 109, 13857–13870.
Pingarron, J.M., Yanez-Sedeno, P., Gonzalez-Cortes, A., 2008. Electrochim. Acta 53, 5848–5866.
Poliakoff, M., Anastas, P., 2001. Nature 413, 257.
Poliakoff, M., Fitzpatrick, J.M., Farren, T.R., Anastas, P.T., 2002. Science 297, 807–810.
Rosi, N.L., Mirkin, C.A., 2005. Chem. Rev. 105, 1547–1562.
Sardar, R., Funston, A.M., Mulvaney, P., Murray, R.W., 2009. Langmuir 25, 13840–13851.
Schmid, G., 1992. Chem. Rev. 92, 1709–1727.
Seo, B., Choi, S., Kim, J., 2011. ACS Appl. Mater. Interfaces 3, 441–446.
Shan, C.S., Yang, H.F., Han, D.X., Zhang, Q.X., Ivaskab, A., Ni, L., 2010. Biosens. Bioelectron. 25, 1070–1074.
Shi, W.T., Ma, Z.F., 2010. Biosens. Bioelectron. 26, 1098–1103.
Somorjai, G.A., 1996. Chem. Rev. 96, 1223–1236.
Sun, X.P., Dong, S.J., Wang, E.K., 2004. Angew. Chem. Int. Ed. 43, 6360–6363.
Sun, X.P., Dong, S.J., Wang, E.K., 2005. Langmuir 21, 4710–4712.
Tan, Y.W., Dai, X.H., Li, Y.F., Zhu, D.B., 2003. J. Mater. Chem. 13, 1069–1075.
Toghill, K.E., Compton, R.G., 2010. Int. J. Electrochem. Sci. 5, 1246–1301.
Tsai, M., Tsai, Y., 2009. Sens. Actuators B 141, 592–598.
Umar, A.A., Oyama, M., 2006. Cryst. Growth Des. 6, 818–821.
Yavuz, M.S., Jensen, G.C., Penaloza, D.P., Seery, T.A.P., Pendergraph, S.A., Rusling, J.F., Sotzing, G.A., 2009. Langmuir 25, 13120–13124.
Yin, A.X., Min, X.Q., Zhang, Y.W., Yan, C.H., 2011. J. Am. Chem. Soc. 133, 3816–3819.
Yin, B.S., Ma, H.Y., Wang, S.Y., Chen, S.H., 2003. J. Phys. Chem. B 107, 8898–8904.